Initial point selection and validation in PS-InSAR using integrated amplitude calibration

Gini Ketelaar, Freek van Leijen, Petar Marinkovic and Ramon Hanssen

Delft Institute of Earth Observation and Space Systems

Delft University of Technology

Kluyverweg 1, 2629HS, Delft, The Netherlands

Telephone: ++31 15 278 2552

Fax: ++31 15 278 3711

Email: v.b.h.ketelaar@lr.tudelft.nl

Abstract— **SAR amplitude calibration is performed prior to the selection of potential Persistent Scatterers (PS) to avoid amplitude variations due to sensor characteristics and viewing geometry. As only the interferometric phases of a small percentage of the radar pixels in an image is used in the PS-InSAR analysis, it is investigated if this time and storage space consuming step can be omitted. We present an integrated method which does not perform amplitude calibration explicitly, but integrates it into the PS point selection procedure for validation purposes by evaluating the hypothesis that a point would have been selected if all images were calibrated beforehand. Its performance assessment is based on coherent phase behavior of the selected potential PS and indicates that empirical calibration validation is an alternative for calibrating full images based on physical sensor parameters.**

I. INTRODUCTION

Persistent Scatterer (PS) [1] InSAR is based on a network of point scatterers with a non-random phase behavior in time. As their interferometric phase contributions due to deformation are obscured by other effects, their identification is based on the amplitude behavior in time. For an unbiased selection of potential PS, a preceding SAR calibration is performed to isolate the amplitude observations corresponding with physical PS properties from amplitude variations due to viewing geometry and sensor characteristics. Since the amount of PS is generally a small percentage of the full image and only their interferometric phase observations are used in the PS-InSAR analysis, the necessity of calibrating full images can be questioned. This study investigates the integration of amplitude calibration in the selection procedure of potential PS as a validation tool to determine if the potential PS would have been selected if the SAR images were calibrated beforehand.

II. INITIAL POINT SELECTION

A. Potential PS parameterization

Several methods are available for potential PS identification:

1) Signal-to-Clutter Ratio (SCR) [2],
2) Amplitude dispersion (D_a) [1],
3) Phase stability [3].

SCR is based on the assumption that an amplitude return is a deterministic signal disturbed by randomly Gaussian distributed clutter. The clutter reflects the distributed scatterers in the surroundings of the potential PS. A point scatterer with a high SCR through time is a potential PS. SCR assumes stationary stochastic behavior of the surroundings, which may not be valid, especially in urban areas with a high PS density. Automatic distinction of two nearby potential PS requires high flexibility of SCR estimation windows and signal edge detectors.

The amplitude dispersion method [1] performs an amplitude time series analysis on an (oversampled) pixel-by-pixel basis. Each pixel is quantified by the ratio between the standard deviation σ_a and the mean μ_a of the amplitudes through time:

$$D_a = \frac{\sigma_a}{\mu_a}. \qquad (1)$$

Point scatterers with a low amplitude dispersion are selected as potential PS. A commonly used threshold is 0.25, which corresponds with a SCR of 8.

Recently phase stability as a selection criterium for potential PS has been investigated [3]. The phase stability is analyzed on the assumption that deformation is spatially correlated, averaging the phases of neighboring potential PS, and selecting the point targets with the lowest residual noise. If potential PS could be detected purely on their phase behavior, SAR calibration could be omitted. However, the selection of these neighboring potential PS is based on amplitude dispersion.

B. PS-InSAR SAR calibration

Both physically related and empirical SAR calibration methods have been investigated to eliminate amplitude variations due to viewing geometry and sensor characteristics. ESA ERS SAR calibration applies system and acquisition dependent corrections to compare backscatter coefficients over the full image [4]. The corrections are applied as a multiplication factor that consists of constant factors (calibration constant, antenna pattern gain, replica pulse power), range dependent factors (slant range, incidence angle) and the powerloss, which varies over the full image. For specific purposes, these corrections can be simplified, resulting in empirical calibration methods. Such an approach for multi-temporal ERS SAR data is described in [5].

For PS-InSAR applications combining different sensors a generalized empirical calibration method can be formulated.

The PS range location variation within the SAR image is limited. Relative SAR calibration of a set of neighboring potential PS in two images can be approximated by a constant factor multiplication. This means that a single master stack of K images is subdivided in grid cells where $K-1$ calibration factors are estimated successively. In case of ERS-2 we may benefit from the knowledge that the intensities are slowly degrading in time [5]. Hence, we only need to estimate the initial factor and the degrading rate. However, the multiplication factors per grid cell are most suitable to generalize the empirical calibration for (a combination of) different sensors.

Understanding the physical implications of the SAR amplitude calibration, it can be deduced that SCR is less affected, as the calibration factor of signal and clutter cancel in the ratio. However, as automatic implementation of SCR is complicated, the SAR amplitude calibration validation is based on D_a. To avoid any a priori assumptions on the (deformation) phase behavior, we limit the potential PS selection to the amplitude sequence. The phase coherence is investigated to assess the performance of the potential PS selection.

III. INTEGRATED SAR CALIBRATION VALIDATION

A. General procedure

The processing strategy to implement SAR calibration validation in PS-InSAR analysis can be summarized as:

1) oversampling with a factor 2 to avoid aliasing,
2) SAR image coregistration to the same radar grid,
3) potential PS subset selection per grid cell based on D_a,
4) calibration parameter estimation and testing,
5) hypothesis testing: would the potential PS have been selected if SAR calibration was performed?

B. Mathematical model

To implement empirical SAR calibration as a validation tool, it is written down as a Gauss-Markov model. Such an approach enables testing of observations, their stochasticity and model assumptions. For a selection of P points within a grid cell, a multiplication factor c_k is estimated relative to a virtual reference image for all K SAR images. The functional and stochastic model read:

$$E\{\underline{y}\} = E\{\underline{a}_p^k\} = c_k a_p^{\text{ref}} \qquad D\{\underline{y}\} = \sum_{p=1}^{P} \sigma_{a_p}^2 Q_p \qquad (2)$$

where $\underline{a}_p^k$ is the amplitude observation for potential PS p in image k with its variance $\sigma_{a_p}^2$. a_p^{ref} is the unknown amplitude for potential PS p free from variations due to sensor characteristics and viewing geometry. After linearization the functional

model reads:

$$E\left\{\begin{bmatrix} \Delta\underline{a}_1^1 \\ \vdots \\ \Delta\underline{a}_1^K \\ \vdots \\ \Delta\underline{a}_P^1 \\ \vdots \\ \Delta\underline{a}_P^K \end{bmatrix}\right\} = \begin{bmatrix} a_1^{\text{ref}0} & & & c^{1^0} & & \\ & \ddots & & & \vdots & \\ & & a_1^{\text{ref}0} & c^{K^0} & & \\ a_P^{\text{ref}0} & & & & & c^{1^0} \\ & \ddots & & & & \vdots \\ & & a_P^{\text{ref}0} & & & c^{K^0} \end{bmatrix} \begin{bmatrix} \Delta c^1 \\ \vdots \\ \Delta c^K \\ \Delta a_1^{\text{ref}} \\ \vdots \\ \Delta a_P^{\text{ref}} \end{bmatrix}$$

$$(3)$$

As calibration factors can only be estimated relatively, a rank defect of 1 has to be resolved, which implies that one calibration factor is fixed at the value 1. It does not matter which calibration factor to fix; the precision of the adjustment results is intrinsically identical. An iterative procedure results in unbiased estimators with minimum variance for the multiplication factors and the unknown reference amplitudes [6].

C. Variance Component Estimation

The observational stochastic model (2) is not very well known a priori. It is assumed that the amplitude variance reflects the independent physical properties of the potential PS superposed with random noise due to viewing geometry (look and squint angle) and atmosphere. Its initial value is the amplitude standard deviation from the uncalibrated stack.

Based on the adjustment residuals, variance factor(s) to update the stochastic model are estimated by Variance Component Estimation (VCE) [7]. In the SAR calibration validation either 1 variance factor $\hat{\sigma}^2$ for the entire variance matrix can be estimated, or a variance factor per potential PS: $\hat{\underline{\sigma}}_1^2 \ldots \hat{\underline{\sigma}}_P^2$.

D. Testing observational errors

Erroneous observations, such as amplitudes of non-stable point scatterers or distributed scatterers, influence the estimates of the calibration factors. Therefore, tests are performed to trace these erroneous observations [8] and remove them from the dataset comparing a null hypothesis H_0 against an alternative hypothesis H_A:

$$H_0 : E\{\underline{y}\} = c_k a_p^{\text{ref}} \qquad \text{versus} \qquad H_A : E\{\underline{y}\} = c_k a_p^{\text{ref}} + C_y \nabla. \tag{4}$$

The matrix C_y specifies the type of potential error and ∇ represents the observational error(s). H_0 is rejected if the teststatistic T_q corresponding with C_y exceeds the critical value k_α.

The following two observational tests are considered:

1) *Datasnooping:* Datasnooping implies successive single amplitude observation tests of dimension 1. For uncorrelated observations $\underline{y}_i$, the teststatistic $\underline{w}_i$ is computed from the residual $\hat{\underline{e}}_i$.

$$\underline{w}_i = \frac{\hat{\underline{e}}_i}{\sigma_{\hat{e}_i}} \qquad c_{y_i} = (0, .., 0, 1_i, 0, .., 0)^T. \tag{5}$$

2) Point test: Tracing single observational errors may be not very efficient, as the aim is to select potential PS. For this reason, an alternative hypothesis is specified to perform an integrated test on all amplitude observations of a single potential PS. Its C matrix reads:

$$C_p = \begin{bmatrix} 0 & \dots & 0 & I_{p\ (K-1)\times(K-1)} & 0 & \dots & 0 \end{bmatrix}^T. \quad (6)$$

The corresponding teststatistic T_{K-1} has dimension $K-1$. For each potential PS, only $K-1$ amplitude observations can be independently combined in an alternative hypothesis. A point test of dimension K would imply the estimation of a constant bias to the amplitude observations, for which the calibration factors are invariant.

E. Tests of different dimensions

When comparing tests of different dimensions, the one with the largest teststatistic should correspond with the most likely alternative hypothesis. However, tests of different dimensions have different probability density functions. Therefore, all tests are performed with a power of 50% and scaled to their critical value. The largest of these teststatistic ratios belongs to the most likely alternative hypothesis.

F. SAR calibration validated potential PS selection

The testing procedure of the amplitude observations and their stochastic model results in calibration factor and reference amplitude estimates plus their precision. The SAR calibration validated selection will consist of the potential PS that fulfill:

$$\frac{\hat{\underline{\sigma}}_{a_p}}{\hat{\underline{a}}_p^{\text{ref}}} < 0.25 \quad (7)$$

where $\hat{\underline{\sigma}}_{a_p}$ is the estimated standard deviation of the amplitude observations of potential PS p and $\hat{\underline{a}}_p^{\text{ref}}$ is its estimated amplitude that is not affected by sensor characteristics.

IV. PERFORMANCE OF SAR CALIBRATION VALIDATION

A. Empirical SAR calibration validation per grid cell

The integrated SAR calibration validation estimates the calibration factors and the reference amplitudes of the best points (25-50) per grid cell. The most optimal way in terms of speed and efficiency is applying point tests for potential PS that do no behave as a point scatterer combined with estimating one variance factor for the stochastic model (Fig. 1). This variance factor is of dual use, as it also quantifies the Overall Model Test (OMT) which is a quality measure of both the functional and the stochastic model.

The mathematical model and the adjustment results are approved when the Overall Model Test equals its expectation value 1 and no more potential PS are rejected. Based on (7) the potential PS are selected that would have passed when the SAR images would have been calibrated beforehand. Fig. 2 shows the amplitude dispersion of the best points within a grid cell for the uncalibrated images and as estimated from the SAR calibration validation procedure. As expected, after
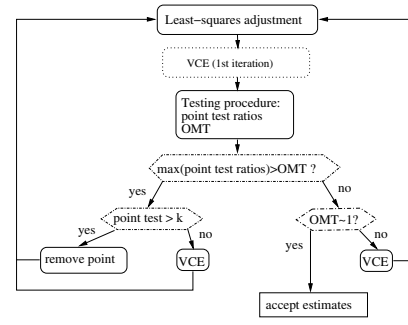
Fig. 1. Adjustment and testing procedure for SAR calibration validation.

SAR calibration validation significantly more potential PS are selected. From the similarity of the amplitude dispersion patterns one could argue that selecting the best points within a grid cell would be sufficient. However, the decrease of the amplitude dispersion is unknown when omitting calibration validation.
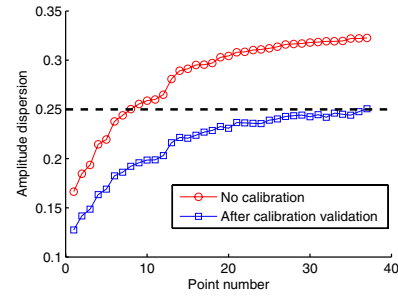
Fig. 2. Estimated amplitude dispersion before and after calibration validation.

Besides the Overall Model Test, an adjustment residual analysis can confirm if the functional and stochastic model are optimal for the unknown parameter estimation. As a point scatterer's amplitude distribution can be approximated by a normal distribution (Fig. 3(a)), the adjustment residuals are normally distributed as well, as they are a linear function of the observations. This is certainly not the case for distributed scatterers.

Fig. 3(b) shows the distribution of all normalized residuals, which are equal to the w-teststatistics (section III-D.1). As can be deduced, the w-teststatistics fit their theoretical standard normal distribution very well. This strengthens the application of the adjustment and testing procedure from Fig. 1.

B. Calibration validation performance based on phase behavior of potential PS

Performance analysis of the integrated SAR calibration validation and comparison to other methods is done based on the phase history of the selected potential PS. The phase residuals per arc between two potential PS are parameterized in a coherence measure. The potential PS is accepted if it is
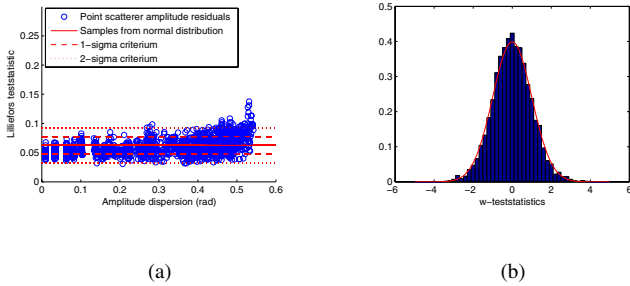
Fig. 3. (a) Goodness-of-Fit to normal distribution of simulated point scatterer amplitude residuals and (b) Distribution of w-teststatistics from real data compared to theoretical distribution.

part of at least two arcs exceeding the phase residual coherence threshold.

For a test area of 4 by 4 kilometers the ESA ERS SAR calibration method has been compared to the integrated SAR calibration validation procedure. A stack of 73 ERS-1 and ERS-2 images were analyzed in the selection of a sparse grid of potential PS for the purpose of the estimation of (residual) topography, deformation, orbital and atmospheric errors. For each grid cell of 200 by 200 meters the best potential PS with the lowest amplitude dispersion below the threshold of 0.25 was selected. Fig. 4 shows the detected potential PS for both the full stack ESA ERS SAR calibration and empirical calibration validation procedure. Table I lists the number of detected potential PS, the percentage of rejected potential PS based on phase behavior (coherence threshold 0.75) and the accepted potential PS in common.
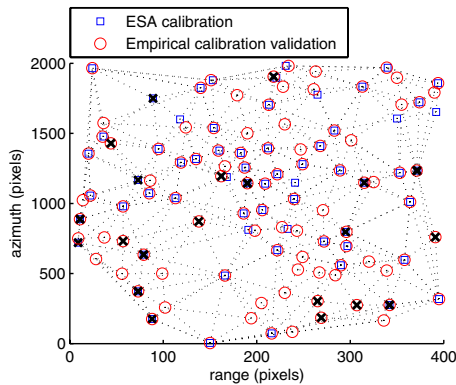
Fig. 4. Detected potential PS for ESA calibration and calibration validation method. Rejected points are marked with a black cross.

TABLE I

COMPARISON OF ESA SAR CALIBRATION AND EMPIRICAL VALIDATION.

	PPS	Rejected	Common PPS
ESA calibration	61	18 %	82 %
Empirical validation	96	19 %	82 %

These results show that for PS-InSAR, a simple empirical

SAR calibration validation is a well performing alternative for calibrating full images based on physical parameters. The false detection rate of both methods is equal, whereas the SAR calibration validation method detects even more potential PS. The number of commonly detected and accepted potential PS is 82%. Especially in grid cells with a high potential PS density, it may occur that the amplitude dispersion of a neighboring point scatterer is slightly higher due to a different estimation procedure. These differences are not caused by coregistration precision, which is for both methods around 0.1 pixel. The higher detection rate of the calibration validation method may possibly be addressed to variability of the estimated calibration factors with Doppler difference. The amplitudes drop for images with a high Doppler frequency [9], which is not taken into account in the ESA ERS SAR calibration.

V. CONCLUSION

For initial point scatterer selection based on amplitudes, it is not necessary to calibrate full SAR images. The most potential point scatterers in terms of amplitude dispersion are utilized in the SAR calibration validation. An adjustment and testing procedure results in estimates for a reference amplitude per potential PS plus its variance and subsequently in an amplitude dispersion not affected by sensor characteristics and viewing geometry. The performance of the SAR calibration validation on real data is analyzed in terms of phase coherence. The results indicate that SAR calibration can be replaced by an empirical calibration validation on a limited selection of scatterers from the uncalibrated stack. Compared to the ESA ERS SAR calibration, it shows a higher flexibility in the test area.

REFERENCES

[1] A. Ferretti, C. Prati, and F. Rocca, "Permanent scatterers in SAR interferometry," *IEEE Transactions on Geoscience and Remote Sensing*, vol. 39, no. 1, pp. 8–20, jan 2001.

[2] in *CEOS SAR Calibration Workshop, ESTEC, Noordwijk, The Netherlands, 20-24 Sept 1993*, 1993.

[3] A. Hooper, H. Zebker, P. Segall, and B. Kampes, "A new method for measuring deformation on volcanoes and other non-urban areas using InSAR Persistent Scatterers," *Geophysical Research Letters*, vol. 31, no. 23, dec 2004.

[4] H. Laur, P. Bally, P. Meadows, J. Sanchez, B. Schaettler, E. Lopinto, and D. Esteban, "Derivation of the backscattering coefficient σ^0 in ESA ERS SAR PRI products," ESA, Tech. Rep. ES-TN-Radio Science-PM-HL09, sep 2002, issue 2, Rev. 5d. [Online].

[5] F. Bovenga, A. Refice, R. Nutricato, G. Pasquariello, and G. DeCarolis, "Automated calibration of multi-temporal ERS SAR data," in *International Geoscience and Remote Sensing Symposium, Toronto, Canada, 24–28 June 2002*, 2002.

[6] P. J. G. Teunissen, *Adjustment theory; an introduction*, 1st ed. Delft: Delft University Press, 2000.

[7] ——, *Towards a Least-Squares Framework for Adjusting and Testing of both Functional and Stochastic Models*, 2nd ed. Delft University of Technology, 1988.

[8] ——, *Testing theory; an introduction*, 1st ed. Delft: Delft University Press, 2000.

[9] B. N. Cassee, "Selection of permanent scatterer candidates for deformation monitoring," MSc thesis, Faculty of Civil Engineering and Geosciences, Delft University of Technology, September 2004.